Supplemental Information

Supplemental Figure Legends

Supplemental Figure 1. No significant difference in the expression of major platelet surface adhesion molecules between *pFn*$^{-/-}$, *Cre*$^{+}$ mice and *pFn*$^{+/+}$, *Cre*$^{-}$ littermates.

Platelet surface expression of adhesion molecules was detected in gel-filtered platelets by flow cytometry. There is no significant difference in platelet surface expression of GPIbβ, β3 integrin (CD61), P-selectin (CD62P), and activated β3 integrin (detected by JON/A antibody) between *pFn*$^{+/+}$ and *pFn*$^{-/-}$ littermates (top panel), between *pFn*$^{+/+}$, *VWF*$^{-/-}$ and *VWF*$^{-/-}$/*pFn*$^{-/-}$ littermates (middle panel), nor between *pFn*$^{+/+}$, *Fg*$^{-/-}$ and *Fg*$^{-/-}$/*pFn*$^{-/-}$ littermates (bottom panel). Platelet surface expression of GPIbβ and β3 integrin was tested in resting platelets. Platelet surface expression of P-selectin and activated β3 integrin was tested in platelets activated with 1 U/mL of thrombin. Solid lines represent *pFn*$^{+/+}$ (*Cre*$^{-}$) mice and dotted lines represent *pFn*$^{-/-}$ (*Cre*$^{+}$) littermates.

Supplemental Figure 2. Prolonged bleeding time in *VWF*$^{-/-}$/*pFn*$^{-/-}$ mice.

For most *VWF*$^{-/-}$ and *VWF*$^{-/-}$/*pFn*$^{-/-}$ mice, tail bleeding cannot stop within 20 min after severing of the tip of the tail. Therefore, instead of cutting the tail, a puncture was made using a 30G needle on one of the tail veins 4 cm from the tip of the tail in *VWF*$^{-/-}$/*pFn*$^{-/-}$ mice and their *Cre*$^{-}$ littermates.

Supplemental Figure 3. pFn purification.

(A) Coomassie Blue staining of pFn purified from *Fg*$^{-/-}$ mice. **(B)** Western blot of pFn purified from two *Fg*$^{-/-}$ mice (1 and 2), pFn from WT mice (WT), commercial mouse pFn (Com), and commercial Fg with anti-Fg antibody. Note that a considerable amount of Fg was present in pFn purified from WT mice and commercial pFn. 1 μg of pFn or Fg was add into each lane. Representative of two independent experiments.

Supplemental Figure 4. pFn deposition.

(A, B) There was no significant difference in the total amount of pFn deposition between *Fg*$^{-/-}$/ *VWF*$^{-/-}$ mice and WT mice after laser injury. **(A)** pFn MFI represents area under the curve (AUC) of the pFn fluorescent intensity in Figure 2C and 2F. **(B)** pFn MFI represents pFn deposition 4 min after injury. **(C)** Persistence of pFn deposition on the injured vessel wall after platelet depletion with monoclonal antibodies. Red: pFn; Green: platelet. **(D)** Marked pFn deposition on collagen was observed 40 seconds after the infusion of purified Alexa Fluor 488-labeled pFn (5 μg/mL) through a collagen-coated glass chamber at a shear rate of 1800 s^{-1}. No labeled BSA (5 μg/mL) deposition was observed in the same perfusion chamber. Scale bars in (C) and (D) represent 10 μm.

Supplemental Figure 5. pFn-fibrin network formation.

(A, B) There was no difference in clot formation velocity (R-time) between *pFn*$^{-/-}$ mice and *pFn*$^{+/+}$, *Cre*$^{-}$ littermates in both whole blood **(A)** and PPP **(B)**. n=6 in each group. **(C)** Co-localization of fibrin and pFn. Confocal images of large bundles of pFn-fibrin network formed in mouse PPP in the TEG cup (z-projection of 11 individual slides taken at 1 μm interval across the 10 μm thickness of the clot). 10 μg of Alexa Fluor 488-labeled Fg and 10 μg of Alexa Fluor 647-labeled pFn were added into PPP prior to clot formation. Scale bars in (C) represent 10 μm.

Supplemental Figure 6. Fg level in *pFn*$^{-/-}$ mice and *pFn*$^{+/+}$, *Cre*$^{-}$ littermates following polyI-polyC injection.

ELISA showed no difference in Fg level between *pFn*$^{-/-}$ and *pFn*$^{+/+}$, *Cre*$^{-}$ littermates following polyI-polyC injection. n=6 in each group.

Supplemental Video Legends

Supplemental Video 1. Plasma fibronectin deposition in cremaster arteriole

Supplemental Video 2. 3D Reconstruction of Plasma fibronectin deposition in mesenteric artery 5 min after injury

Supplemental Video 3. Plasma fibronectin deposition on collagen in perfusion chamber

Supplemental Table 1. No significant difference in the blood cell counts between *Cre*$^{+}$ mice and *Cre*$^{-}$ littermates.

Genotype	***pFn*$^{+/+}$**	***pFn*$^{-/-}$**	**P**
RBC (x 10^{-9}/mL)	10.23 ± 0.46	10.28 ± 1.06	0.947
WBC (x 10^{-6}/mL)	13.00 ± 2.58	9.75 ± 3.86	0.218
PLT (x 10^{-6}/mL)	760 ± 139	711 ± 242	0.736
Genotype	***pFn*$^{+/+}$, *VWF*$^{-/-}$**	***VWF*$^{-/-}$/*pFn*$^{-/-}$**	**P**
RBC (x 10^{-9}/mL)	9.07 ± 1.45	10.25 ± 1.42	0.337
WBC (x 10^{-6}/mL)	10.00 ± 3.16	15.25 ± 7.27	0.255
PLT (x 10^{-6}/mL)	628 ± 168	853 ± 268	0.213
Genotype	***pFn*$^{+/+}$, *Fg*$^{-/-}$**	***Fg*$^{-/-}$/*pFn*$^{-/-}$**	**P**
RBC (x 10^{-9}/mL)	10.48 ± 1.33	10.68 ± 0.99	0.818
WBC (x 10^{-6}/mL)	8.25 ± 3.30	11.50 ± 5.05	0.448
PLT (x 10^{-6}/mL)	656 ± 103	751 ± 207	0.454

There was no significant difference in the blood cell counts between *Cre*$^{+}$ mice and *Cre*$^{-}$ littermates. N=4 in each group. Data shown as mean ± SD. P value was calculated by unpaired Student t-test.

Supplemental Experimental Procedures

Materials

DyLight 649 and DyLight 488 fluorescent labeled anti-GPIb antibodies and JON/A (antibody against mouse-activated GPIIbIIIa) were purchased from Emfret Analytics. Alexa Fluor 488 and Alexa Fluor 647 protein labeling kits were purchased from Life Technologies Inc. Human Fg was purchased from Sigma-Aldrich. Recombinant hirudin (r-hirudin) was provided by Dr. Jawed Fareed at Loyola University, Chicago.

Mice

pFn conditional deficient ($Fn^{flox/flox}$, $Cre^{+/-}$) mice, VWF deficient ($VWF^{-/-}$) mice, Fg deficient ($Fg^{-/-}$) mice, and VWF, Fg, and pFn triple deficient (TKO, $VWF^{-/-}/Fg^{-/-}$, $Fn^{flox/flox}$, $Cre^{+/-}$) mice were previously described (1-4). In these mice, part of the fibronectin gene is flanked by loxP sites ($Fn^{flox/flox}$). They also contain the *Mx-cre* transgene, which upon activation with polyinonic-polycytidylic acid (polyI-polyC; Sigma-Aldrich) injection, leads to the deletion of part of the fibronectin gene and arrest of its expression. β3 integrin deficient ($\beta3^{-/-}$) mice were provided by Dr. Richard O. Hynes (Howard Hughes Medical Institute, Massachusetts Institute of Technology, Boston, MA) (5). Syngeneic C57BL/6J mice were purchased from The Jackson Laboratory.

$VWF^{-/-}/pFn^{-/-}$ mice were generated by breeding male $VWF^{-/-}$ mice with female $pFn^{-/-}$ mice. $VWF^{-/-}$, $Fn^{flox/flox}$, $Cre^{+/-}$ mice were used to generate $VWF^{-/-}$, $Fn^{flox/flox}$, Cre^{+} and $VWF^{-/-}$, $Fn^{flox/flox}$, Cre^{-} littermates. $Fg^{-/-}/pFn^{-/-}$ mice were generated by breeding male $Fg^{-/-}$ mice with female $pFn^{-/-}$ mice. Uterine bleeding causes female $Fg^{-/-}$ mice mortality during pregnancy (3); therefore, female $Fg^{+/-}$, $Fn^{flox/flox}$, $Cre^{+/-}$ mice and male $Fg^{-/-}$, $Fn^{flox/flox}$, $Cre^{+/-}$ mice were bred to produce $Fg^{-/-}$, $Fn^{flox/flox}$, Cre^{+} and $Fg^{-/-}$, $Fn^{flox/flox}$, Cre^{-} littermates. pFn depletion was induced by three intraperitoneal injections of 250 μg of polyI-polyC into both the Cre^{+} and Cre^{-} littermates at two-day intervals. Mouse

genotypes were determined using polymerase chain reaction and confirmed by Western blot. Depletion of pFn in the plasma and platelets was confirmed by Western blot analysis. The condition of the mice was monitored daily following polyI-polyC injection. Autopsies were performed on deceased mice.

Bleeding time

The bleeding time assay was modified from the procedure previously described (6). 6-8 week-old mice were anesthetized with 2.5% tribromoethanol (0.015ml/g) and maintained at 37°C on a heating pad throughout the experiment. The tip of the tail (2 mm) was cut off with a sharp scalpel. For most *VWF*$^{-/-}$ and *VWF*$^{-/-}$*/pFn*$^{-/-}$ mice, tail bleeding cannot stop within 20 min after severing of the tip of the tail. Therefore, instead of cutting the tail, a puncture was made using a 30G needle on one of the tail veins 4 cm from the tip of the tail in *VWF*$^{-/-}$ and *VWF*$^{-/-}$*/pFn*$^{-/-}$ mice. The injured tail was immediately placed into warm PBS at 37°C. The bleeding time was recorded from the time of injury until 10 seconds after the bleeding had ceased. For the transfusion study, PBS (200 μL), purified pFn solution (1.5 mg/mL, 200 μL), or BSA (1.5 mg/mL, 200 μL, biotechnology grade, Wisent Inc) were injected via the tail vein 30 min before bleeding time was assessed. For the anticoagulant study, PBS (200 μL), heparin (100 Unit/mL, 200 μL, Pharmaceutical Partners of Canada), or r-hirudin (0.5 mg/kg, 200 μL) were injected intraperitoneally 30 min before the bleeding time assay. Bleeding time assay was terminated at 20 min, and mice that bled beyond this end point were counted as 20 min. For mice transfused with 200 μL of PBS, pFn or BSA, we extended the end point of the tail bleeding assay to 30 min.

Preparation of mouse plasma and platelets

Mouse plasma and platelets were prepared as previously described (4, 7, 8). Mice (6-8 weeks old) were anesthetized and bled from the retroorbital plexus with heparin-coated glass capillary tubes. For in vitro pFn-fibrin clot formation, blood was drawn from the inferior vena cava (IVC) with a

25G needle. The blood was immediately mixed with 3.2% sodium citrate (1/9, vol/vol). Platelet-rich plasma (PRP) was prepared by centrifugation at 300 ×g for 7 min. Platelet-poor plasma (PPP) was prepared by centrifugation at 1500 ×g for 20 min. Gel-filtered platelets were prepared from the PRP with a Sepharose 2B column in PIPES buffer (PIPES 5 mM, NaCl 1.37 mM, KCl 4 mM, glucose 0.1%, pH 7.0).

Detection of platelet surface adhesive proteins and peripheral blood count

Platelet surface adhesive proteins were detected with flow cytometry as described previously (4). Gel-filtered Cre^+ and Cre^- platelets were examined for platelet surface expression of GPIbβ, β3 integrin (CD61), and P-selectin (CD62P) and for activation of β3 integrin (detected by JON/A antibody). Resting gel-filtered platelets (10^6) from Cre^+ and Cre^- mice were incubated separately with a 1:100 dilution of PE-conjugated rat anti-mouse CD61 (BD Pharmingen). GPIbβ was detected using 10 μg/mL rat anti-mouse GPIbβ antibody (DyLight 488; EMFRET Analytics). Platelet surface P-selectin expression was detected on resting or thrombin-treated (1 U/mL) platelets after incubation with FITC-conjugated rat anti-mouse CD62P (BD Pharmingen). To examine the activation of β3 integrin, thrombin-treated (1 U/mL) platelets were incubated with R-phycoerthrin-conjugated JON/A antibody (JON/A-PE; EMFRET Analytics), an antibody that recognizes only activated mouse αIIbβ3 integrin. All samples were analyzed by a FACScan flow cytometer (BD Biosciences).

To determine the peripheral blood cell counts in mice, 20 μL of whole blood was collected into an EDTA-coated microvette from each polyI-polyC-treated Cre^+ and Cre^- control mouse. Peripheral blood cell counts were analyzed with a HEMAVET HV950FS (Drew Scientific) counter.

Purification and fluorescent labeling of mouse and human pFn

pFn was isolated using gelatin-sepharose chromatography. Briefly, fresh $Fg^{-/-}$ mouse PPP or human

PPP was loaded onto a gelatin-sepharose 4B (GE Healthcare) column. The medium was then washed with PBS until protein was undetectable in the collected washing buffer. pFn was then eluted with 8M urea. The pFn urea solution was dialyzed against PBS overnight at 4°C. The purity of pFn was evaluated with Coomassie Blue protein staining. 1 μg of pFn or Fg was applied to each lane on the SDS gel. The presence of Fg in pFn purified from *Fg*$^{-/-}$ mice, from WT mice, and from a commercial mouse pFn product (Molecular Innovations) were tested with Western blot using a rabbit anti-human Fg antibody (American Diagnostica). Human plasma Fg (Sigma-Aldrich) was used as a positive control. The Alexa Fluor 488 or 647 protein labeling kit (Invitrogen) was used for mouse and human pFn labeling.

Intravital microscopy thrombosis model

Laser-induced cremaster arterial thrombosis was performed as previously described (4, 9, 10). Briefly, male adult mice were anesthetized and a tracheal tube was inserted to facilitate breathing. Anesthetic reagents (pentobarbital, 0.05 mg/kg, Abbott Laboratories) were administered through a jugular vein cannula. Platelet depletion was achieved by injection of p0p9 antibodies (Provided by Dr. Bernhard Nieswandt, University of Würzburg, Würzburg, Germany). The cremaster muscle was prepared under a dissecting microscope and superfused throughout the experiment with preheated bicarbonate-buffered saline. Alexa Fluor 488-labeled pFn (5 μg) and DyLight 649 anti-GPIb antibodies (1 μg per 1 g body weight, Emfret) were injected through the jugular vein cannula prior to injury. For detection of fibrin formation, an Alexa Fluor 488-labeled mouse anti-human fibrin IIβ chain antibody (2 μg/g body weight, Accurate Chemical) was injected prior to laser injury. Multiple independent injuries were induced on cremaster arterioles using an Olympus BX51W1 microscope with a pulsed nitrogen dye laser. The dynamic deposition of pFn onto the injured vessel wall and the formation of the hemostatic plug were captured and analyzed using Slidebook software (Intelligent Imaging Innovations).

Confocal microscopy study

The $FeCl_3$ injury mesenteric arterial model was described previously (7). After injection of Alexa Fluor 647-labeled pFn (5 μg) and DyLight 488 anti-GPIb antibodies (1 μg/g body weight, Emfret) through the tail vein, the mice were anesthetized and mid-abdominal incisions were made. The intestines were pulled out in order to expose the mesenteric arteries. Injury to the mesenteric arteries was induced by topical application of 30 μL of 250 mM $FeCl_3$. pFn deposition and thrombus formation were recorded by a Zeiss LSM 700 confocal laser scanning microscopy (Zeiss). The confocal data were analyzed by ZEN 2010 software (Zeiss) and the 3D reconstruction of the image was produced by Imaris x64 (Bitplane). Identical microscopy and software settings were applied for all experiments.

Perfusion chamber analysis

For the pFn deposition study, Alexa Fluor 488-labeled pFn (5 μg/mL) or BSA (5 μg/mL) was perfused over the collagen-coated glass chamber surface (microcapillary glass tube coated with 100 μg/mL Horm collagen (Nycomed) overnight) at a controlled shear rate (1800 s^{-1}) for 3 min using a syringe pump. pFn deposition was recorded by an inverted fluorescent microscope (Axiovert 135, Zeiss). For the thrombus formation study, heparin (5 U/mL) anti-coagulated whole blood from $pFn^{+/+}$, $Fg^{-/-}$ mice or $Fg^{-/-}/pFn^{-/-}$ mice was perfused over the collagen-coated glass chamber surface at a controlled shear rate (1800 s^{-1}) for 3 min using a syringe pump. The thrombus formation was captured by a confocal microscopy (CARV confocal cell imaging, BD biosciences). The volume of the thrombi was analyzed using Slidebook software (Intelligent Imaging Innovations).

Detection of Fg by enzyme-linked immunosorbent assay

PPP (100 μL) from $pFn^{-/-}$ mice and $pFn^{+/+}$ mice was incubated in wells overnight at 4°C. After washing and blocking with BSA, a rabbit anti-human Fg antibody (American Diagnostica) was added to the plates and incubated for 2 hours. After 5 washes, a conjugated goat anti-rabbit

secondary antibody (Sigma-Aldrich) was added and incubated for 2 hours. Substrate was added for 30 min after 5 washes. The reaction was terminated and the samples were read at 540 nm in an ELISA plate reader (Bio-Tek Instruments). PPP from *Fg*$^{-/-}$ mice was used as a negative control. OD value measured in *Fg*$^{-/-}$ PPP was subtracted from the value measured in *pFn*$^{-/-}$ and *pFn*$^{+/+}$ PPP.

Thromboelastography

Blood was obtained from mouse IVC with a 25G needle and immediately mixed with 3.2% sodium citrate in a 9:1 ratio. The whole blood or PPP was tested in a TEG 5000 Analyzer (Hemoscope). 340 µL fresh blood was mixed with 20 µL 0.2 M $CaCl_2$ at the beginning of each experiment. For the coagulation of PPP, 330 µL PPP was pre-activated with kaolin and mixed with 30 µL 0.2 M $CaCl_2$. The tests were halted after clot forming parameters were calculated, or after 1.5h, whichever occurred first. Specific clot forming parameters were obtained from the resultant hemostasis profile: R time, which represents the period of latency from the time the blood was placed in the TEG analyzer until initial fibrin network formation (bifurcation of the tracing), and maximum amplitude (MA), which reflects the maximum strength of the platelet-fibrin clot. For imaging of the pFn-fibrin fibers formed in TEG, 10 µg Alexa Fluor 488-labeled Fg and 10 µg Alexa Fluor 647-labeled pFn were premixed with mouse PPP. The clot was removed from the TEG cups after termination of the experiment and observed under an inverted fluorescent microscope (Axiovert 135, Zeiss). The images shown are z-projections of 11 individual planes taken at 1 µm interval across the 10 µm thickness of the clot.

pFn-fibrin network formation in vitro

In vitro pFn-fibrin network formation was performed with modified procedure as previously described (11). 90 µL *pFn*$^{-/-}$ PPP was premixed with 10 µL of Alexa Fluor 488-labeled Fg (1 mg/mL, Sigma-Aldrich). 50 µL pFn (45 µL unlabeled pFn and 5 µL Alexa Fluor 647-labeled pFn, both at 1 mg/mL) or 50 µL BSA (45 µL unlabeled BSA and 5 µL Alexa Fluor 647-labeled BSA,

both at 1 mg/mL, biotechnology grade, Wisent Inc) was then added to the 100 μL PPP aliquots. The solution was mixed with $CaCl_2$ (30 mM) and murine thrombin (0.5 U/mL, Sigma-Aldrich) and immediately transferred to a Sigmacote-treated (Sigma-Aldrich) glass chamber. The clotting process took around 1 min to form a homogenous 10 μm thick clot. The samples were then observed under a Zeiss LSM 700 confocal laser scanning microscope (Zeiss). For experiments with human plasma, human PPP was applied to the gelatin column. The plasma passing through the gelatin column was tested by Western blot and was found to have a minimal pFn level. The pFn-depleted human PPP was used for human pFn-fibrin network formation in vitro.

Scanning electron microscopy

100 μL $pFn^{-/-}$ PPP was mixed with 50 μL pFn (1 mg/mL), BSA (1 mg/mL), or PBS. The mixture was clotted with $CaCl_2$ (30 mM) and murine thrombin (0.5 U/mL, Sigma-Aldrich) and immediately transferred to a Sigmacote-treated (Sigma-Aldrich) glass chamber. For pFn-fibrin network formation in $pFn^{+/+}$ and $pFn^{-/-}$ mice, $pFn^{+/+}$ or $pFn^{-/-}$ PPP was directly clotted with $CaCl_2$ (30 mM) and murine thrombin (0.5 U/mL, Sigma-Aldrich). The samples were fixed in 3% glutaraldehyde and processed for scanning electron microscopy (S-2500, Hitachi). The calculated diameter of the pFn-fibrin fibers was the average diameter of all fibers crossed by two diagonal lines drawn on the image. The density was the total number of fibers crossed by the two diagonal lines in a 1 μm^2 square. Average diameter and density were calculated from nine or ten independent experiments.

In vitro platelet aggregation

Platelets were prepared and aggregation was assayed as previously described (4, 8, 10). Platelet concentration in PRP or PIPES buffer was adjusted to 3×10^8 platelets/mL with autologous PPP or PIPES buffer, respectively. Platelet aggregation in PRP or PIPES buffer was induced by various agonists, including 20 μM ADP (Sigma-Aldrich), 20 μg/mL collagen (Nycomed), 0.2 U/mL murine thrombin (Sigma-Aldrich), or 500 μM thrombin receptor activating peptide (TRAP; AYPGKF-NH_2;

Peptides Int.). Platelet aggregation was monitored and recorded with a computerized aggregometer (Chrono-Log) with the stir bar rate set to 1000 rpm at 37°C.

Statistical analysis

Data were presented as mean plus or minus SEM. Statistical significance was assessed by the Student unpaired t test (two-tailed) or the χ^2 test with Yates' correction. $P < 0.05$ was considered statistically significant. For statistical analysis of anticoagulant treated mice in which none of them could stop bleeding, 95% confidence interval of bleeding time in the control group (which could stop bleeding) was calculated for the determination of statistical significance.

Study Approval

All animal studies were approved by the Animal Care Committee of St. Michael's Hospital, Toronto. All experimental procedures using human plasma were approved by the Research Ethics Board of St. Michael's Hospital, Toronto. Human blood samples were drawn from antecubital veins of healthy volunteers after providing informed consent according to guidelines provided by Research Ethics Board of St. Michael's Hospital, Toronto.

References

1. Sakai T, Johnson KJ, Murozono M, Sakai K, Magnuson MA, Wieloch T, Cronberg T, Isshiki A, Erickson HP, and Fassler R. Plasma fibronectin supports neuronal survival and reduces brain injury following transient focal cerebral ischemia but is not essential for skin-wound healing and hemostasis. *Nat Med.* 2001;7(3):324-30.
2. Denis C, Methia N, Frenette PS, Rayburn H, Ullman-Cullere M, Hynes RO, and Wagner DD. A mouse model of severe von Willebrand disease: defects in hemostasis and thrombosis. *Proc Natl Acad Sci U S A.* 1998;95(16):9524-9.
3. Suh TT, Holmback K, Jensen NJ, Daugherty CC, Small K, Simon DI, Potter S, and Degen JL. Resolution of spontaneous bleeding events but failure of pregnancy in fibrinogen-deficient mice. *Genes Dev.* 1995;9(16):2020-33.
4. Reheman A, Yang H, Zhu G, Jin W, He F, Spring CM, Bai X, Gross PL, Freedman J, and Ni H. Plasma fibronectin depletion enhances platelet aggregation and thrombus formation in mice lacking fibrinogen and von Willebrand factor. *Blood.* 2009;113(8):1809-17.
5. Hodivala-Dilke KM, McHugh KP, Tsakiris DA, Rayburn H, Crowley D, Ullman-Cullere M, Ross FP, Coller BS, Teitelbaum S, and Hynes RO. Beta3-integrin-deficient mice are a model for Glanzmann thrombasthenia showing placental defects and reduced survival. *J Clin Invest.* 1999;103(2):229-38.
6. Chen J, Reheman A, Gushiken FC, Nolasco L, Fu X, Moake JL, Ni H, and Lopez JA. N-acetylcysteine reduces the size and activity of von Willebrand factor in human plasma and mice. *J Clin Invest.* 2011;121(2):593-603.
7. Ni H, Denis CV, Subbarao S, Degen JL, Sato TN, Hynes RO, and Wagner DD. Persistence of platelet thrombus formation in arterioles of mice lacking both von Willebrand factor and fibrinogen. *J Clin Invest.* 2000;106(3):385-92.
8. Yang H, Reheman A, Chen P, Zhu G, Hynes RO, Freedman J, Wagner DD, and Ni H. Fibrinogen and von Willebrand factor-independent platelet aggregation in vitro and in vivo. *J Thromb Haemost.* 2006;4(10):2230-7.
9. Falati S, Gross P, Merrill-Skoloff G, Furie BC, and Furie B. Real-time in vivo imaging of platelets, tissue factor and fibrin during arterial thrombus formation in the mouse. *Nat Med.* 2002;8(10):1175-81.
10. Reheman A, Gross P, Yang H, Chen P, Allen D, Leytin V, Freedman J, and Ni H. Vitronectin stabilizes thrombi and vessel occlusion but plays a dual role in platelet aggregation. *J Thromb Haemost.* 2005;3(5):875-83.
11. Campbell RA, Overmyer KA, Selzman CH, Sheridan BC, and Wolberg AS. Contributions of extravascular and intravascular cells to fibrin network formation, structure, and stability. *Blood.* 2009;114(23):4886-96.

Supplemental Figure 1.

Gel-filtered platelets

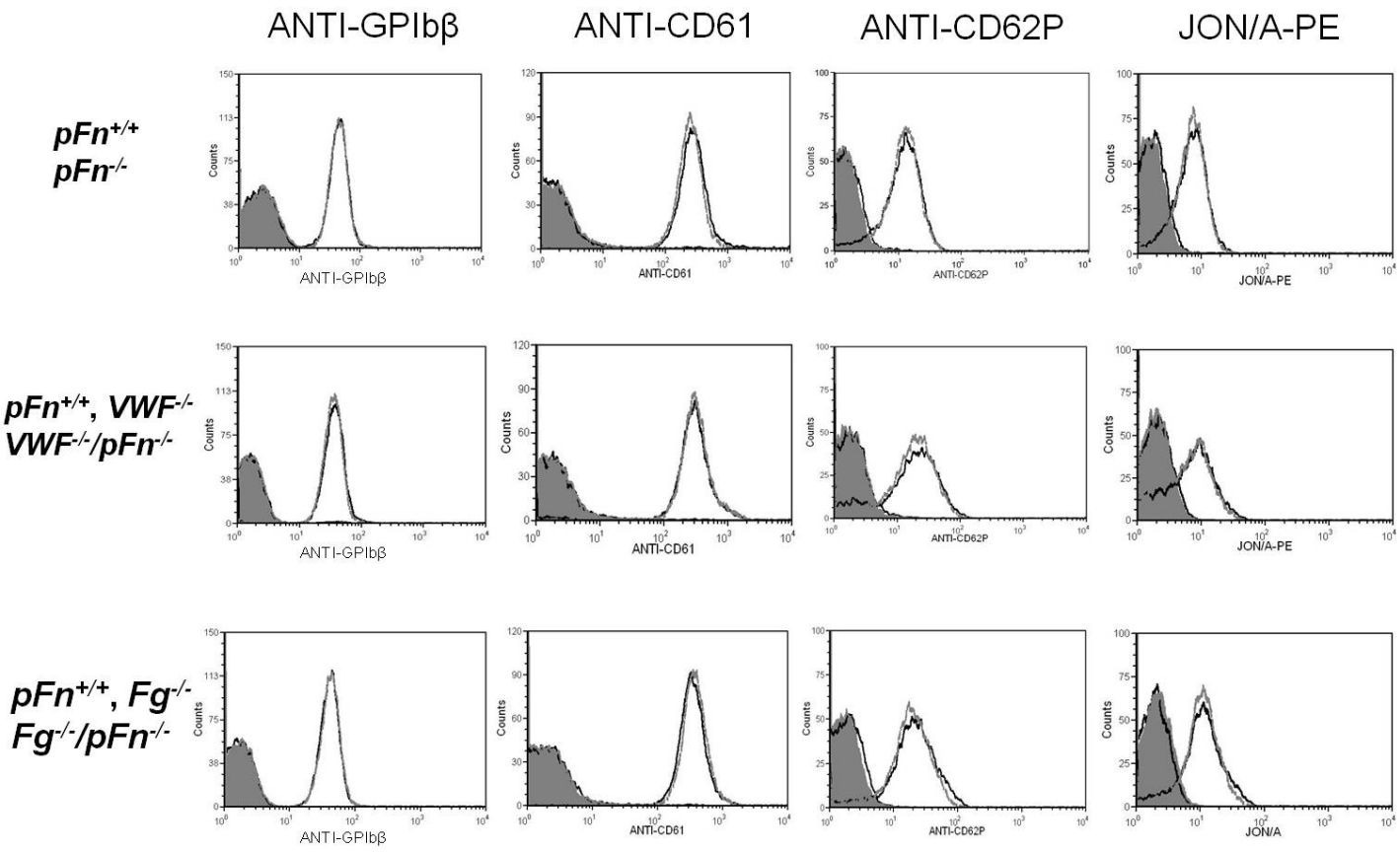

Supplemental Figure 2.

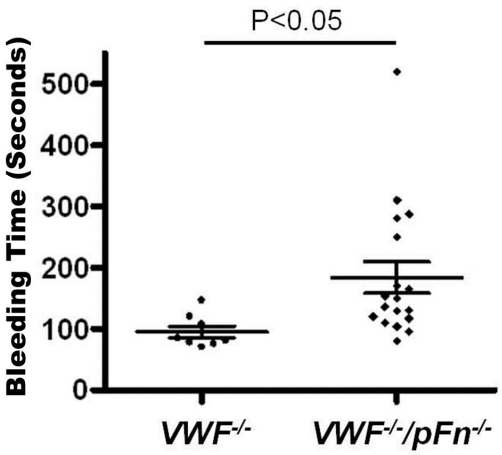

Supplemental Figure 3.

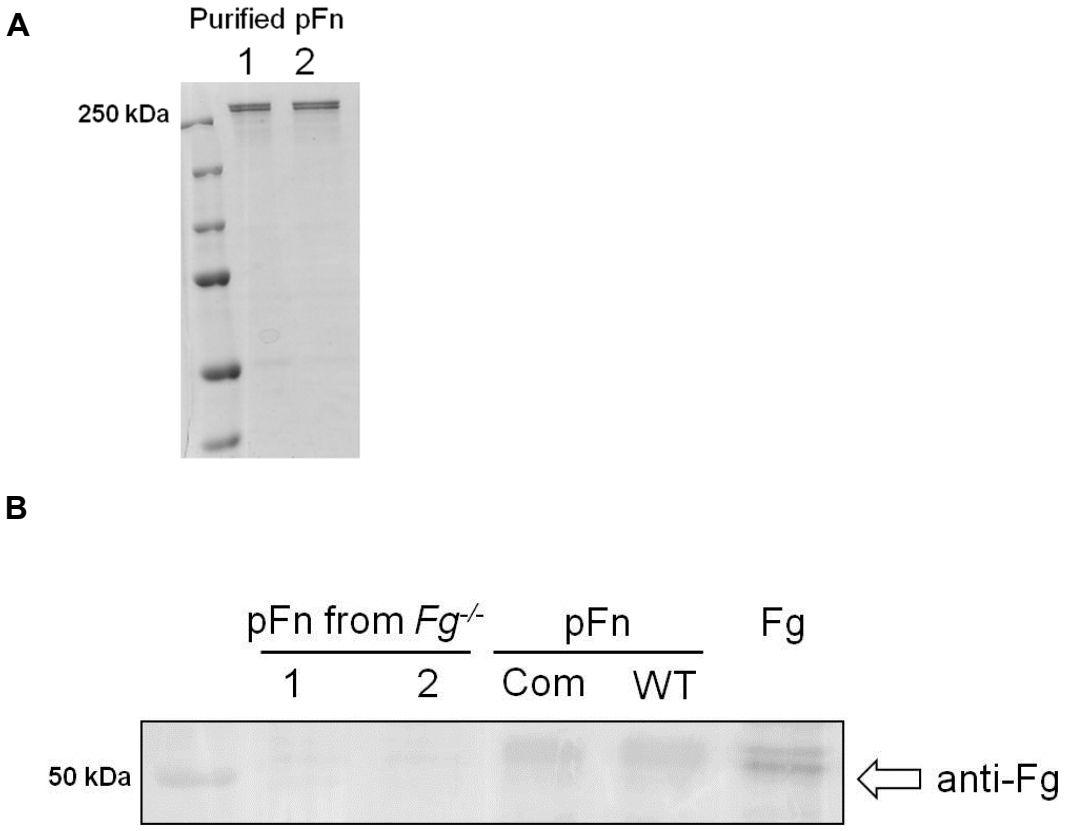

Supplemental Figure 4.

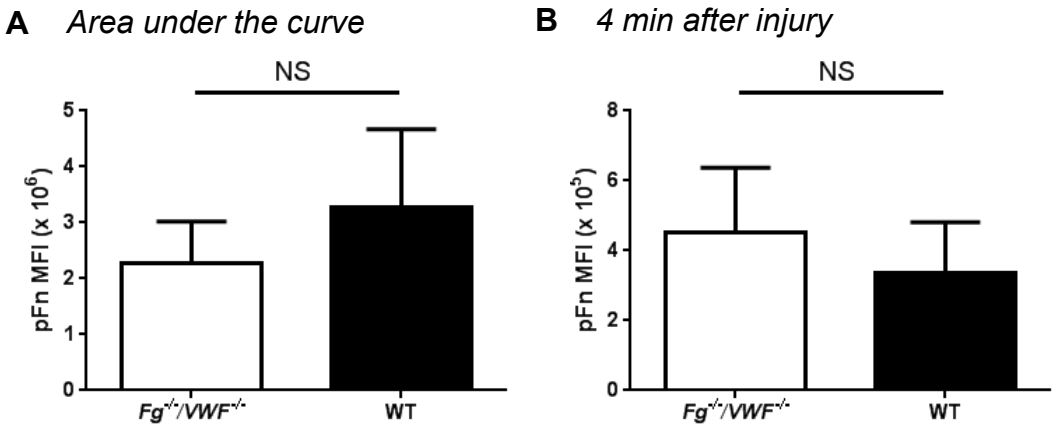

C

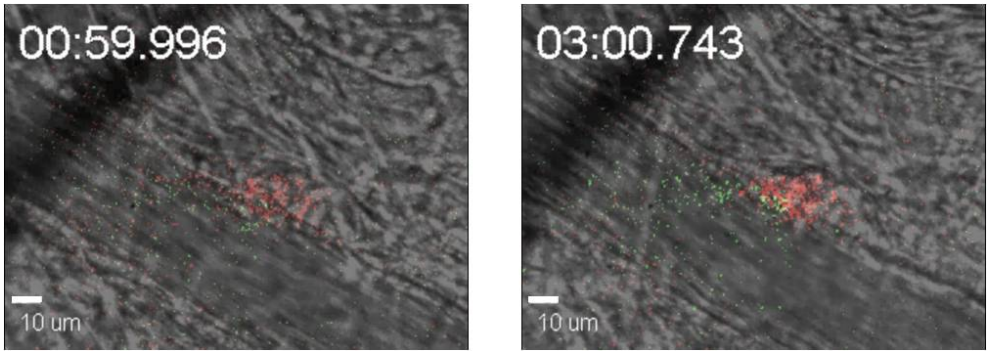

D

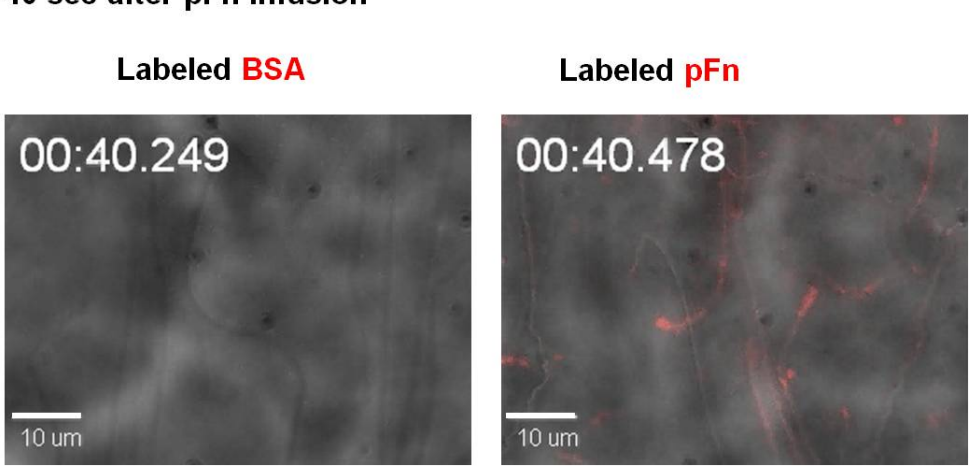

Supplemental Figure 5.

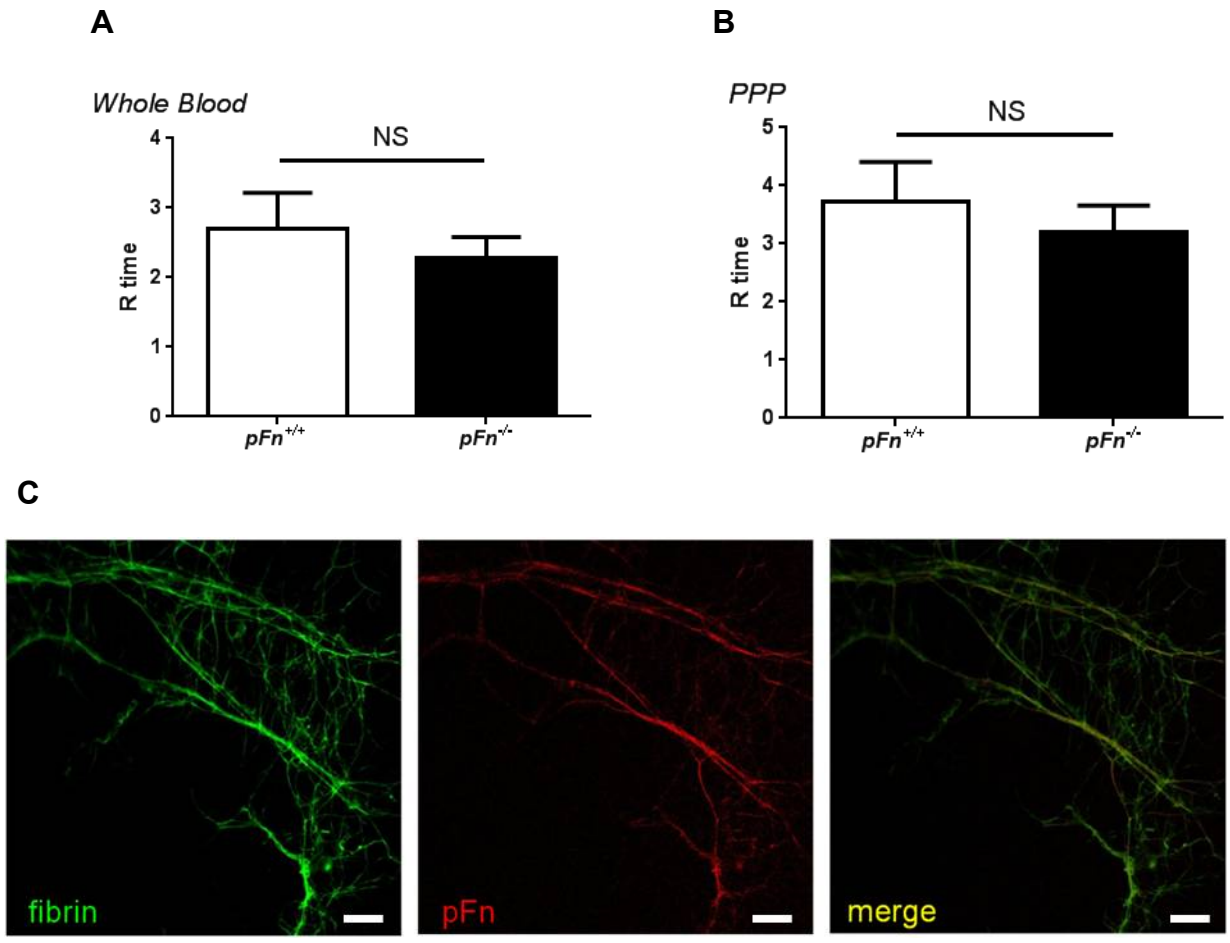
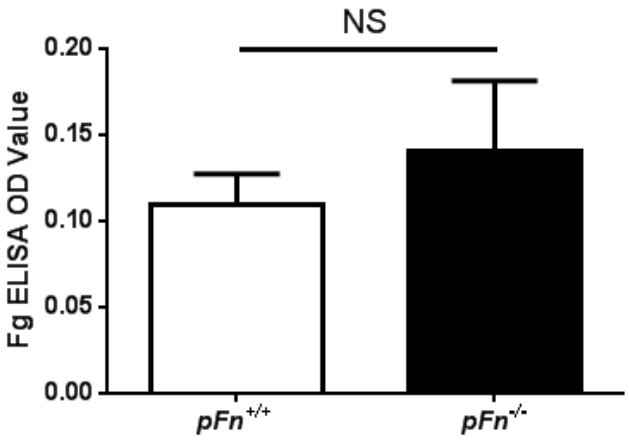
Supplemental Figure 6.